

# Anomaly detection on cup anemometers

Enrique Vega, Santiago Pindado, Alejandro Martínez, Encarnación Mesequer and Luis García

## Abstract

The performances of two rotor-damaged commercial anemometers (Vector Instruments A100 LK) were studied. The calibration results (i.e. the transfer function) were very linear, the aerodynamic behavior being more efficient than the one shown by both anemometers equipped with undamaged rotors. No detection of the anomaly (the rotors' damage) was possible based on the calibration results. However, the Fourier analysis clearly revealed this anomaly.

## 1. Introduction

Anemometer degradation is a well-known problem in the wind energy industry. As a cup anemometer loses performance, due to the normal wear and tear process or due to sudden incidents such as lightning, the wind speed measurement given by the instrument diverges from the real wind speed. As a consequence, this effect can be translated into a wrong wind turbine operation or inaccurate data when studying the energy production of a specific geographic location, causing a negative impact on the revenue. As aforementioned, this is not a new problem either for the wind energy sector or in meteorology. Furthermore, it can be said that around 30% of mast-mounted anemometers return for recalibration far from normal operational conditions [1].

Currently, the only solution for keeping anemometers in proper working condition is to check them through frequent calibrations [2]. However, the process of taking the anemometer to the calibration facility can be unaffordable in terms of cost and is time-consuming. Calibration-on-the-field procedures have been studied as a cost-effective solution for reducing anemometer maintenance and the number of recalibrations [3, 4]. In addition, to illustrate the considerable interest of the industry in this matter, several patents and inventions have been developed in an attempt to solve this problem [5–13].

Besides the maintenance problem (recalibration, change of parts, etc), it can be even more important to know, as precisely as possible, when a cup anemometer which is working on the field, requires some maintenance. This can be considered an example of the anomaly detection problem. In the industry, anomaly detection is usually addressed through three different approaches: case-based reasoning, model-based diagnosis and non-parametric models [14]. Regarding loss of performance in cup anemometers, the results of the PHM 2011 Data Challenge Competition are particularly interesting. In the competition, the working condition of several cup anemometers had to be analyzed, comparing the data from paired units installed along a vertical mast [15–17].

In the current work, an anomaly detection process developed at the IDR/UPM Institute [18] is applied, for the first time, to two commercial cup anemometers (Vector Instruments A100 LK) with damaged rotors after a quite a long period of service. The performance of these Class-1 anemometers is analyzed and compared to the performance of the same type of anemometers, but equipped with undamaged rotors. The main advantage of the developed methodology is in its simplicity, as the working condition of the cup anemometer is only based on the data from its output signal, with no comparison with a second anemometer dataset required.

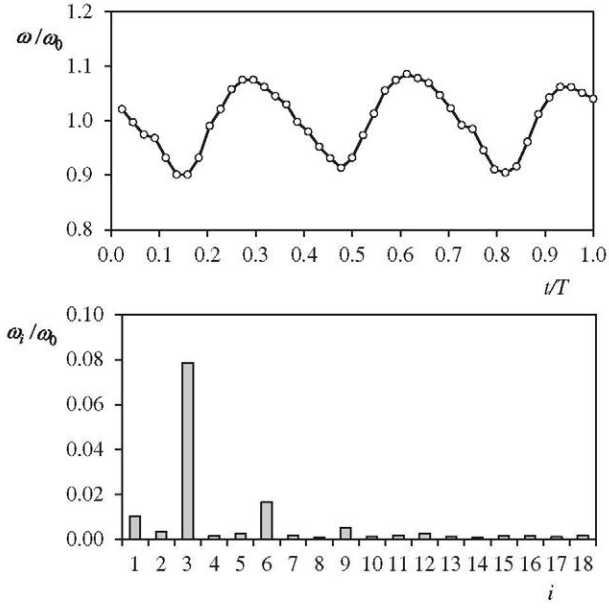


**Figure 1.** Relative-to-the-average rotational speed,  $\omega/\omega_0$ , of a Thies anemometer during one turn at  $8 \text{ m s}^{-1}$  wind speed [29] (top) and non-dimensional values of the Fourier series expansion performed at that rotational speed,  $\omega_i/\omega_0$  (bottom).

The results included in this work are part of a full research program carried out since 2011 at the IDR/UPM Institute regarding the cup anemometer performance, which covers a large series of calibration analyses [19], rotor aerodynamics [20–22], the effect of climatic conditions [23] or the ageing problem [24].

The current work is organized as follows. In section 2 the calibration and post-processing process are described. The results are discussed in section 3 and the conclusions are summarized in section 4.

## 2. Testing configuration and cases studied

The cup anemometer performance is commonly evaluated through the transfer function:

$$V = A \cdot f + B, \quad (1)$$

that gives the wind speed,  $V$ , as a function of the output frequency of the anemometer,  $f$ . The slope and offset ( $A$  and  $B$ , respectively) of the above equation have to be defined by a proper calibration process. The transfer function can also be defined in terms of rotational frequency,  $f_r$ , instead of output frequency,  $f$ :

$$V = A_r \cdot f_r + B. \quad (2)$$

This new slope,  $A_r$ , being the result of multiplying calibration constant  $A$  by the number of pulses per turn,  $N_p$ , given by the anemometer [19]. The calibration process performed on the anemometers studied follows MEASNET [25, 26] recommendations (over 13 points and from 4 to  $16 \text{ m s}^{-1}$  wind speed). At each point (wind speed) of every calibration performed, the anemometer's output was sampled during 20 s

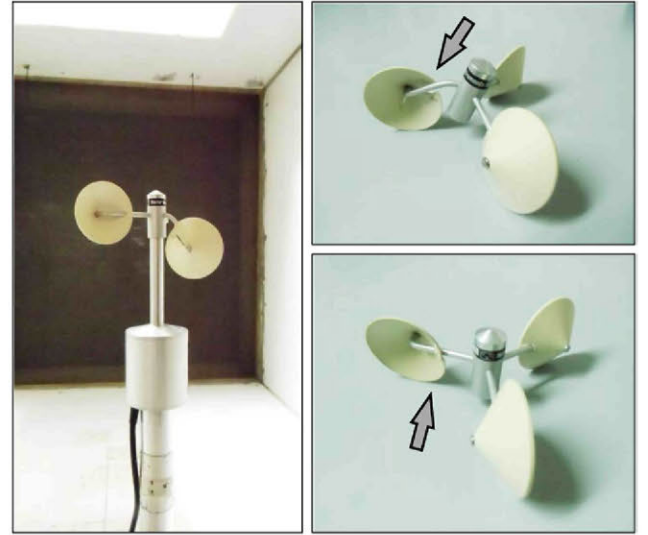


**Figure 2.** Anemometer 1 at the IDR/UPM calibration wind tunnel (left). Damaged rotor of Anemometer 1 (top right) and Anemometer 2 (bottom right).

at 10000 Hz. The first nine harmonic terms of the rotational speed Fourier expansion:

$$\begin{aligned} \omega(t) = & \omega_0 + \omega_1 \sin(\omega_0 t + \varphi_1) + \omega_2 \sin(2\omega_0 t + \varphi_2) \\ & + \omega_3 \sin(3\omega_0 t + \varphi_3) \dots = \omega_0 + \sum_{n=1}^{\infty} \omega_n \sin(n\omega_0 t + \varphi_n) \end{aligned} \quad (3)$$

were calculated in each sampling of the output signal. In order to characterize the anemometer harmonic performance, averaged values of the non-dimensional harmonic terms,  $\bar{\omega}_i$ , were calculated with data from the 13 points of each calibration procedure:

$$\bar{\omega}_i = \frac{1}{13} \sum_{j=1}^{13} \frac{\omega_i}{\omega_0} \Big|_j. \quad (4)$$

See in figure 1 an example of the Fourier expansion (i.e. the terms in relation to the averaged rotation speed) derived from a commercial cup anemometer output signal. More information about this harmonic characterization of a cup anemometer can be found at [20].

Anemometer calibrations of the study cases were performed in the S4 wind tunnel at the IDR/UPM Institute. This is an open-circuit wind tunnel with a closed test section measuring 0.9 by 0.9 m. It is served by four 7.5 kW fans with a flow uniformity better than 0.2% in the testing area. The wind speed in the testing chamber is measured by an Airflow 0.48 Pitot tube connected to a Druck LPM 9481 high-precision pressure transducer, with the electrical signal from the pressure transducer measured by a Keithley 2000 digital multimeter. Temperature and humidity sensors (Vaisala PTU 200 and Vaisala HMP45D) are used to determine the air density value. The rotation frequency of the anemometer is measured with an Agilent 53131A universal counter. Another digital multimeter is used to measure the voltage or current output from the anemometer when required. The uncertainty levels of the calibrations performed at the S4 calibration wind tunnel are

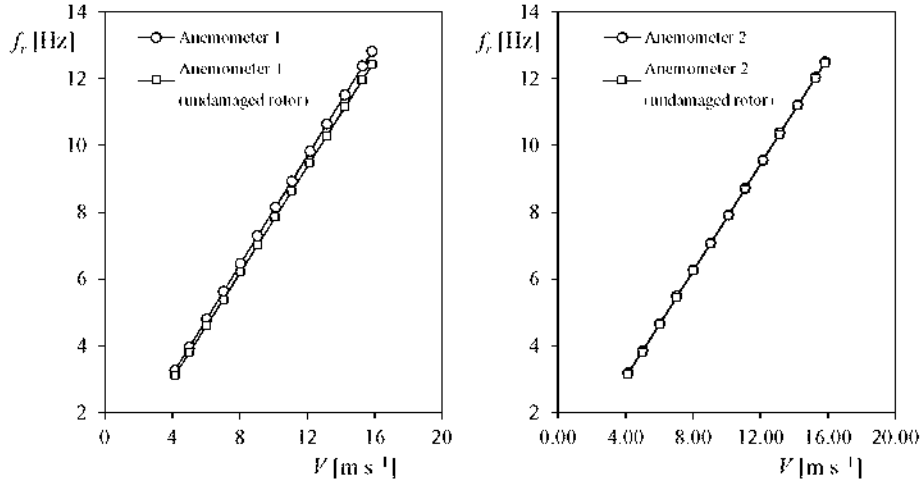


**Figure 3.** Rotation frequency,  $f_r$ , of Anemometer 1 and Anemometer 2 plotted as a function of the wind speed,  $V$ . The results regarding both anemometers equipped with undamaged rotors have been included in the graphs.

specified following the ISO/IEC 17025 standard [27], these levels being  $0.1 \text{ m s}^{-1}$  for wind speeds from 4 to  $10 \text{ m s}^{-1}$  and  $0.01V \text{ m s}^{-1}$  for wind speeds,  $V$ , from 10 to  $23 \text{ m s}^{-1}$ . More information regarding the anemometer calibration processes at the IDR/UPM Institute can be found at [19, 22, 28].

As indicated in the previous section, two Vector Instruments A100 LK cup anemometers were studied, both being damaged after being in service on the field. See in figure 2 pictures of the state of the rotors. The rotor of the first anemometer, herein after denoted as Anemometer 1, is heavily damaged, with one cup completely out of position, whereas the second one, hereinafter denoted as Anemometer 2, is less damaged.

### 3. Results

In figure 3, the rotation frequency,  $f_r$ , corresponding to the calibrations performed on both anemometers, Anemometer 1 and Anemometer 2, is plotted as a function of the wind speed,  $V$ . In addition, the results corresponding to additional calibrations performed on both anemometers now equipped with undamaged rotors are included in the graphs. As can be observed in figure 3, the results of the calibrations were successfully linear (with correlation coefficients above 0.99999, according to MEASNET procedures [25, 26]).

Besides, the percentage difference between the rotational frequency,  $f_r$ , of each anemometer equipped with its damaged rotor and equipped with the undamaged rotor,  $f_r|_{\text{ndr}}$ , calculated in relation to the first one:

$$\Delta f_r = \frac{f_r - f_r|_{\text{ndr}}}{f_r} \quad (5)$$

is plotted as a function of the wind speed,  $V$ , in figure 4.

The results are quite surprising, as the damage effect on the rotor seems to increase (in both anemometers) the rotation rate, i.e. the aerodynamic efficiency of the rotor (see figure 4). The possible explanation for these results lies in the new position of the damaged cups within the rotors. In Anemometer 1, the damaged cup is out of the wake produced by the other

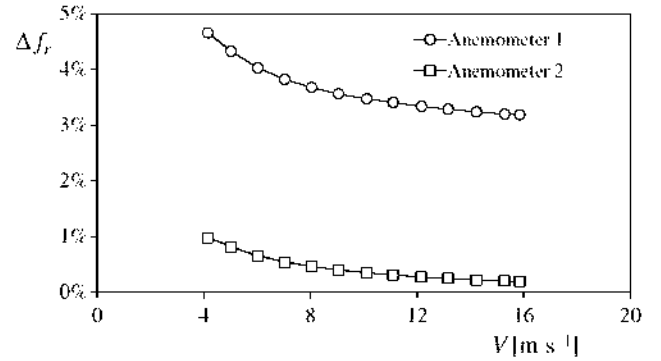


**Figure 4.** Percentage difference,  $\Delta f_r$ , between the rotational frequency,  $f_r$ , of each anemometer equipped with its damaged rotor and equipped with the undamaged rotor,  $f_r|_{\text{ndr}}$ , calculated in relation to the first one.

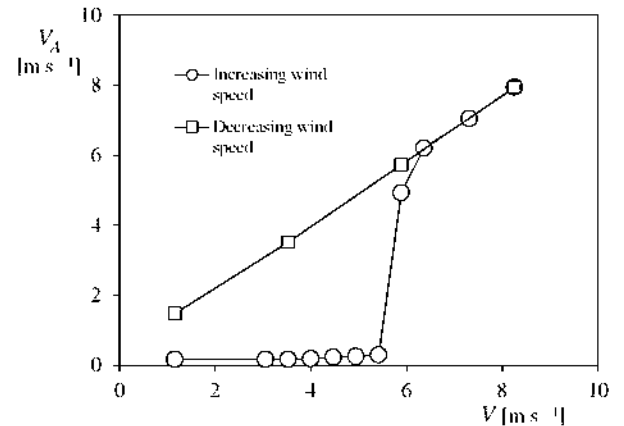


**Figure 5.** Wind speed measured by Anemometer 1,  $V_A$ , as a function of the wind speed,  $V$ , in two different situations: increasing wind speeds from  $V = 1.158$  to  $V = 7.949 \text{ m s}^{-1}$  and decreasing wind speeds starting from  $V = 7.949$  to  $V = 1.158 \text{ m s}^{-1}$ .

cups, whereas one of these is less affected by any wake, as the damaged cup is not aligned with the rotor plane anymore. As one of the cups is now closer to the rotation axis, the decrease of the rotor's moment of inertia obviously produces higher

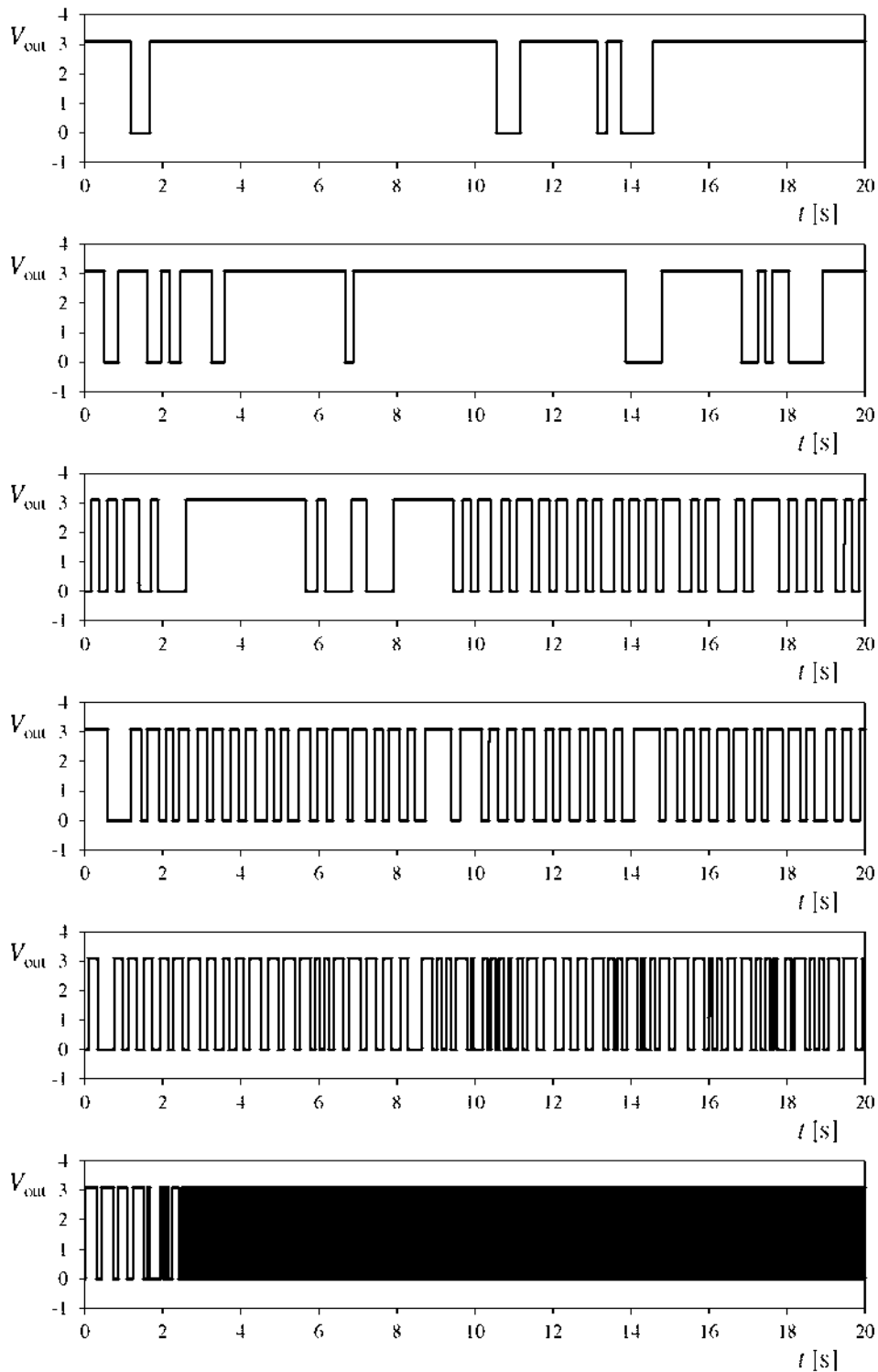


**Figure 6.** Voltage output,  $V_{out}$ , of Anemometer 1 during 20s, for (from top to bottom)  $V = 3.524, 3.997, 4.470, 4.944, 5.417$  and  $5.890\text{m s}^{-1}$  wind speed.

rotation speeds. In order to check this behavior, the calibration performed with the anemometer equipped with the damaged rotor was repeated after three days, with identical results.

On the other hand, although the case of Anemometer 2 is different, with a damaged cup in alignment with the other two, it can be observed that the damaged cup has a slight tilt angle when compared to the other cups in the rotor. It should be

pointed out that tilted cups have been recently introduced in some cup anemometers such as Thies Clima 4.3351 [30]. In addition, in other patents regarding anemometer tilted cups [31], these rotors are claimed to have a higher rotation speed when compared with non-tilted cups rotors.

Reverting to the anomaly detection problem, it should be pointed out that it is very difficult to find out if a cup

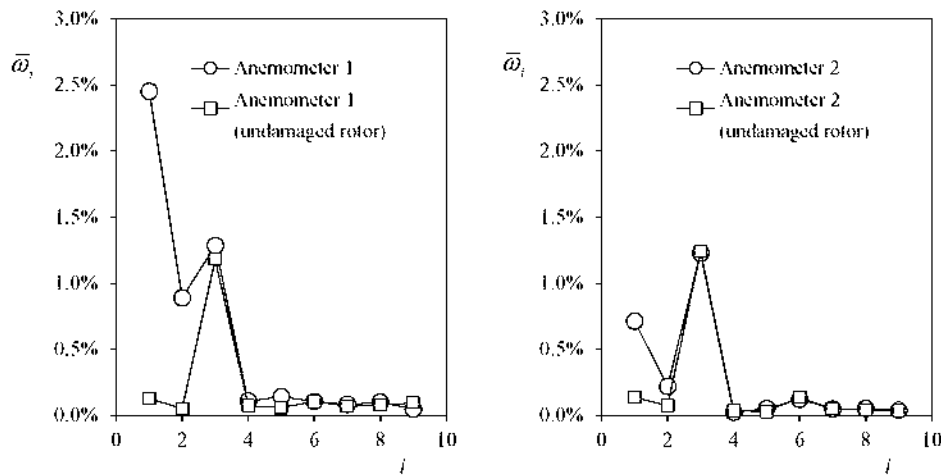


**Figure 7.** Non-dimensional averaged harmonic terms calculated from the Fourier series decomposition of the rotational speed of Anemometer 1 and Anemometer 2. See expression (3). The harmonic terms regarding both anemometers equipped with undamaged rotors have been included in the graphs.

anemometer is damaged based only on the linearity of the calibration results. As previously stated, both anemometers studied were clearly damaged, showed linear transfer functions and somehow a better aerodynamic behavior than the one measured with an undamaged rotor. Nevertheless, even showing a good performance during the calibration process, Anemometer 1 was clearly affected by the rotor damage, which, having changed its size, also modifies the aerodynamics. As a result, a stable equilibrium state (that is, the rotor does not move and remains at a fixed position) is produced at low wind speed, which is translated into quite a high starting threshold speed. In figure 5, the measured wind speed of Anemometer 1,  $V_A$ , is plotted as a function of the wind speed,  $V$ , in two different situations, for increasing wind speeds from  $V = 1.158$  to  $V = 7.949 \text{ m s}^{-1}$  and for decreasing wind speeds starting from  $V = 7.949$  to  $V = 1.158 \text{ m s}^{-1}$ . It can be observed in the figure that the starting threshold speed is around  $V = 5.890 \text{ m s}^{-1}$ , whereas the starting speed specified by the manufacturer is  $V = 0.2 \text{ m s}^{-1}$ . Furthermore, it should be noted that even in this equilibrium state at low wind speeds, Anemometer 1 can give false measurements produced by the oscillations of the rotor produced as a result of its interaction with the turbulent wake created downstream from the anemometer's 'neck' (Vector Instruments A100 L.K anemometers are equipped with a 25 pulse per turn opto-electronic output signal system [19], therefore, a slight rotor oscillation can produce a train of pulses). In figure 6, the voltage output of the anemometer during 20 s is plotted for  $V = 3.524, 3.997, 4.470, 4.944, 5.417$  and  $5.890 \text{ m s}^{-1}$  wind speed, while the rotor was oscillating at the equilibrium position. In the figure, it can be appreciated that, as the wind speed increases, the oscillations of the rotor produce a higher number of pulses. Therefore, a false measurement of the wind speed is recorded by the system. Finally, the transition from the oscillating equilibrium state to the rotation state of Anemometer 1 at  $V = 5.890 \text{ m s}^{-1}$  (i.e. when the anemometer rotor starts to rotate, generating a much higher pulse frequency), can be observed in the bottom graph of figure 6.

One solution in order to detect anemometer anomalies properly comes from the Fourier analysis of the output signal, not directly, but by studying the harmonic terms in each rotation as indicated in section 2. In figure 7, the results of the aforementioned harmonic analysis are shown. Both anemometers, Anemometer 1 and Anemometer 2, present a high value of the first harmonic term,  $\bar{\omega}_1$ , in comparison with the figures presented by both anemometers when equipped with undamaged rotors. This first harmonic term theoretically reflects perturbations on the anemometer rotor's rotation that are repeated in every turn [18]. Therefore, any non-axisymmetric detail of the rotor geometry might produce an aerodynamic perturbation in each turn. The results agree with this statement; the damage on the rotor being perfectly reflected in the graphs of figure 7 when compared to the results related to the undamaged rotors.

#### 4. Conclusions

The performance of two damaged-on-the-field Class-1 cup anemometers (Vector Instruments A100 L.K) has been studied. The most significant conclusions resulting from this work are:

- Damaged rotors can produce a more efficient aerodynamic behavior when compared to undamaged rotors.
- Damaged-rotor anemometers can show a perfectly linear transfer function. However, they might also change the anemometer starting threshold speed.
- The proposed Fourier analysis is capable of detecting the aerodynamic anomalies/perturbations produced by non-axisymmetric damage on cup rotors of commercial anemometers equipped with opto-electronic output signal systems.

#### Acknowledgments

The authors gratefully acknowledge Prof Ángel Sanz-Andrés for his encouraging support regarding the research program on cup anemometer performance and David Carrión and Brian

Elder for their assistance in improving the style of the text. Prof Pindado and the co-authors are indebted to the staff of the Library at the Aeronautics and Space Engineering School (Escuela de Ingeniería Aeronáutica y del Espacio) of the Polytechnic University of Madrid (Universidad Politécnica de Madrid), for their constant support for the research carried out regarding cup anemometer performance. The authors are also grateful to STE Global Spain for their kind support.

- Stefanatos N, Papadopoulos P, Binopoulos E, Kostakos A and Spyridakis G 2007 Effects of long term operation on the performance characteristics of cup anemometers *European Wind Energy Conf. and Exhibition EWEC 2007 (7–10 May, Milan, Italy)* pp 1–6
- Papadopoulos K H, Stefanatos N C, Paulsen U S and Morfiadakis E 2001 Effects of turbulence and flow inclination on the performance of cup anemometers in the field *Boundary-Layer Meteorol.* **101** 77–107
- Kristensen L, Jensen G, Hansen A and Kirkegaard P 2001 *Field Calibration of Cup Anemometers* Risø National Laboratory Report Risø-R-1218(EN) (Roskilde, Denmark)
- Paulsen U S, Mortensen N G, Hansen J C, Said U S and Mousa A S 2007 Field calibration of cup anemometers *European Wind Energy Conf. and Exhibition (7–10 May 2007, Milan, Italy)* pp 1–8
- Corten G P 2001 Method for testing an anemometer *Patent* WO 2001035109 A1
- Ema H, Fumio H, Masato W, Yasuhide T, Hitoshi K, Yasuo T, Mitsuo O and Mitsuhiro I 1998 Testing apparatus and method for anemometer *Patent* JP 10227810 A
- Frost J S, Haines D A and Klumpp R J 1982 Method and apparatus for field testing of anemometers *Patent* US 4365504 A
- Laguigne D and Roni-Damon B 2010 Procédé et dispositif pour vérifier le bon fonctionnement d'un anémomètre (Method and device to check the correct operation of an anemometer) *Patent* EP 2 037 284 B1
- Cummings D S 2011 Apparatus and calibration method for cup anemometers having non-removable cupsets *Patent* US 20110283766 A1
- Beltrán J, Llombart A and Guerrero J 2009 A bin method with data range selection for detection of nacelle anemometers faults *Proc. European Wind Energy Conf. and Exhibition (EWEC) (16–19 March 2009, Marseille, France)* pp 1–8
- Beltrán J, Llombart A and Guerrero J 2009 Detection of nacelle anemometers faults in a wind farm *Proc. Int. Conf. on Renewable Energies and Power Quality (ICREPQ 2009) (15–17 April 2009, Valencia, Spain)* pp 1–6
- Siebers T, Kooijman H-J and Rogers D 2008 Anemometer calibration method and wind turbine *Patent* US 20080307853 A1
- Wobben A 2010 Method for monitoring a sensor *Patent* EP 1454058 A1
- Desforges M J, Jacob P J and Cooper J E 1998 Applications of probability density estimation to the detection of abnormal conditions in engineering *Proc. Inst. Mech. Eng. C* **212** 687–703
- Cassidy J, Aven C and Parker D 2012 Applying weibull distribution and discriminant function techniques to predict damaged cup anemometers in the 2011 PHM Competition *Int. J. Progn. Health Manag.* **3** 1–7
- Siegel D and Lee J 2011 An auto-associative residual processing and k-means clustering approach for anemometer health assessment *Int. J. Progn. Health Manag.* **2** 50–61
- Sun L, Chen C and Cheng Q 2012 Feature extraction and pattern identification for anemometer condition diagnosis *Int. J. Progn. Health Manag.* **3** 8–18
- Pindado S, Cubas J and Sorribes-Palmer F 2014 On the harmonic analysis of cup anemometer rotation speed: a principle to monitor performance and maintenance status of rotating meteorological sensors *Measurement* submitted
- Pindado S, Vega E, Martínez A, Meseguer E, Franchini S and Pérez I 2011 Analysis of calibration results from cup and propeller anemometers. Influence on wind turbine annual energy production (AEP) calculations *Wind Energy* **14** 119–32
- Pindado S, Cubas J and Sanz-Andrés A 2013 Aerodynamic analysis of cup anemometers performance. The stationary harmonic response *Sci. World J.* **2013** 197325
- Pindado S, Pérez J and Avila-Sanchez S 2012 On cup anemometer rotor aerodynamics *Sensors (Basel)* **12** 6198–217
- Pindado S, Pérez I and Aguado M 2013 Fourier analysis of the aerodynamic behavior of cup anemometers *Meas. Sci. Technol.* **24** 065802
- Pindado S, Sanz A and Wery A 2012 Deviation of cup and propeller anemometer calibration results with air density *Energies* **5** 683–701
- Pindado S, Barrero-Gil A and Sanz A 2012 Cup anemometers' loss of performance due to ageing processes, and its effect on annual energy production (AEP) estimates *Energies* **5** 1664–85
- MEASNET 1997 Cup anemometer calibration procedure Version 1 (September 1997, updated 24/11/2008) (Madrid, Spain)
- MEASNET 2009 Anemometer calibration procedure, Version 2 (October 2009) (Madrid, Spain)
- ENAC 2012 Anexo Técnico. Acreditación No 134 / LC10. 095. INSTITUTO UNIVERSITARIO DE MICROGRAVEDAD 'IGNACIO DA RIVA' (available at: <http://www.enac.es/documents/7020/67cfa73f-f539-4c13-8172-986daad8514a>; accessed on 29 January 2014)
- Sanz-Andrés A, Pindado S and Sorribes F 2014 Mathematical analysis of the effect of the rotor geometry on cup anemometer response *Sci. World J.* **2014** 537813
- Dahlberg J-Å, Pedersen T F and Busche P 2006 *ACCUWIND—Methods for Classification of Cup Anemometers* Risø National Laboratory Report Risø-R-1555(EN) (Roskilde, Denmark)
- Schmoling L and Straten G 2006 Rotational anemometer *Patent* EP 1 398 637 B1
- Hong S-H 2011 Asymmetric-cup anemometer *Patent* US 2012/0266692 A1